1   **Identification of key determinants of *Staphylococcus aureus* vaginal colonization**

2

3   RUNNING TITLE: **Characterization of *S. aureus* vaginal colonization**

4

5   Liwen Deng[1,2], Katrin Schilcher[1], Lindsey R. Burcham[1], Jakub M. Kwiecinski[1], Paige M.

6   Johsnon[1], Steven R. Head[3], David E. Heinrichs[4], Alexander R. Horswill[1,5*], Kelly S. Doran[1,2*]

7

8   [1]Department of Immunology and Microbiology, University of Colorado School of Medicine,

9   Aurora, CO, USA.

10   [2]Department of Cell and Molecular Biology, San Diego State University, San Diego, CA, USA.

11   [3]Next Generation Sequencing Core, The Scripps Research Institute, La Jolla, CA, USA.

12   [4]Department of Microbiology and Immunology, University of Western Ontario, London,

13   Ontario, Canada.

14   [5]Department of Veterans Affairs Eastern Colorado Healthcare System, Aurora, Colorado, USA.

15

16   *Corresponding authors: Alexander R. Horswill and Kelly S. Doran, Department of Immunology

17   and Microbiology, University of Colorado School of Medicine, 12800 East 19th Avenue Aurora,

18   CO, USA.

19   Phone: (303) 724-3539, Fax: (303) 724-4226, E-mail: alexander.horswill@cuanschutz.edu,

20   kelly.doran@cuanschutz.edu

21

ABSTRACT

Staphylococcus aureus is an important pathogen responsible for nosocomial and community acquired infections in humans, and methicillin-resistant *S. aureus* (MRSA) infections have continued to increase despite wide-spread preventative measures. *S. aureus* can colonize the female vaginal tract and reports have suggested an increase in MRSA infections in pregnant and postpartum women as well as outbreaks in newborn nurseries. Currently, little is known about specific factors that promote MRSA vaginal colonization and subsequent infection. To study *S. aureus* colonization of the female reproductive tract in a mammalian system, we developed a mouse model of *S. aureus* vaginal carriage and demonstrated that both hospital-associated and community-associated MRSA isolates can colonize the murine vaginal tract. Immunohistochemical analysis revealed an increase in neutrophils in the vaginal lumen during MRSA colonization. Additionally, we observed that a mutant lacking fibrinogen binding adhesins exhibited decreased persistence within the mouse vagina. To further identify novel factors that promote vaginal colonization, we performed RNA-sequencing to determine the transcriptome of MRSA growing *in vivo* during vaginal carriage at 5 hours, 1-day, and 3-days post-inoculation. Over 25% of bacterial genes were differentially regulated at all time points during colonization compared to laboratory cultures. The most highly induced genes were those involved in iron acquisition, including the Isd system and siderophore transport systems. Mutants deficient in these pathways did not persist as well during *in vivo* colonization. These results reveal that fibrinogen binding as well as the capacity to overcome host nutritional limitation are important determinants of MRSA vaginal colonization.

IMPORTANCE

45   *Staphylococcus aureus* is an opportunistic pathogen able to cause a wide variety of

46   infections in humans. Recent reports have suggested an increasing prevalence of MRSA in

47   pregnant and postpartum women, coinciding with the increased incidence of MRSA infections in

48   the NICU and newborn nurseries. Vertical transmission from mothers to infants at delivery is a

49   likely route of MRSA acquisition by the newborn, however, essentially nothing is known about

50   host and bacterial factors that influence MRSA carriage in the vagina. Here, we established a

51   mouse model of vaginal colonization and observed that multiple MRSA strains can persist in the

52   vaginal tract. Additionally, we determined that MRSA interactions with fibrinogen as well as

53   iron uptake can promote vaginal persistence. This study is the first to identify molecular

54   mechanisms which govern vaginal colonization by MRSA, the critical initial step preceding

55   infection and neonatal transmission.

56

57   **INTRODUCTION**

58   *Staphylococcus aureus* is a commensal of approximately 20% of the healthy adult

59   population (1) and also an opportunistic bacterial pathogen able to cause a wide variety of

60   infections ranging in severity from superficial skin lesions to more serious invasive and life-

61   threatening infections such as endocarditis and septicemia. Prevalence of *S. aureus* infections has

62   increased due to higher rates of colonization, immunosuppressive conditions, greater use of

63   surgical implants, and dramatic increases in antibiotic resistance (2, 3). Compared to antibiotic-

64   susceptible strains, methicillin-resistant *S. aureus* (MRSA) infections exhibit elevated mortality

65   rates, require longer hospital stays, and exert a higher financial burden on patients and healthcare

66   institutions (4). Over the past 20 years, MRSA strains have expanded from healthcare settings

67   and began infecting otherwise healthy individuals in the community ("community-associated"

68   MRSA (CA-MRSA))(5). USA300 isolates are the most problematic lineage of CA-MRSA that

69   have emerged and clonally expanded across the US, reaching epidemic levels in many hospital

70   settings (6, 7).

71   Methicillin-susceptible *S. aureus* and MRSA possesses many virulence factors that

72   promote bacterial persistence and invasive infections in different host sites. These virulence

73   factors include cell wall-anchored surface proteins that facilitate *S. aureus* adherence to and

74   invasion of host cells (8), proteases that modulate the host immune response to the bacterium (9),

75   as well as pore-forming toxins such as α-toxin and the bicomponent leukocidins that lyse host

76   cells (10). The expression of these various virulence determinants is dependent on factors such as

77   growth rate, the availability of certain nutrients, host interactions, and the presence of

78   antimicrobial compounds (8, 11-13).

79   Nasal carriage is known to be a risk factor for *S. aureus* infections both in the hospital

80   and in the community with individuals often being infected with the strain that they carry (14).

81   *S. aureus* can colonize the moist squamous epithelium in the anterior nares (15, 16), a process

82   which depends upon specific interactions between bacterial cell adhesins and epithelial cell

83   ligands. Two *S. aureus* surface proteins, clumping factor B (ClfB) and iron regulated surface

84   determinant A (IsdA), have been strongly implicated in nasal colonization. Both ClfB and IsdA

85   were shown to promote adhesion to nasal epithelium *in vitro* (17) and colonization of the nares

86   of rodents (18, 19) and, in the case of ClfB, humans (20). ClfB is a member of a family of

87   proteins that are structurally related to clumping factor A (ClfA), the archetypal fibrinogen (Fg)

88   binding protein of *S. aureus*. ClfB has been shown to bind Fg, as well as cytokeratin 10, by the

89   "dock, lock, and latch" mechanism first defined for the Fg binding proteins SdrG and ClfA (21,

90   22). Additional surface proteins shown to contribute to bacterial attachment to nasal epithelial

4

91   cells *in vitro* include *S. aureus* surface protein G (SasG) and the serine-aspartate repeat proteins

92   SdrC and SdrD (23).

93   While a ubiquitous colonizer of the skin and mucous membranes, *S. aureus,* including

94   antibiotic sensitive and resistant strains, has also been reported to colonize the vagina in up to

95   22% of pregnant women (24-29). A study that examined MRSA colonization showed that out of

96   5,732 mothers, 3.5% were colonized by MRSA in the genital tract during pregnancy (24).

97   Another recent study of 1834 mothers showed that 4.7% were colonized vaginally by multidrug-

98   resistant *S. aureus* (30). Reports have suggested an increasing prevalence in the USA300 lineage

99   of MRSA in pregnant and postpartum women, coinciding with the increased incidence in the

100   NICU and in newborn nurseries (31-36). MRSA outbreaks in NICUs can be difficult to control

101   and have been associated with significant morbidity and mortality (33). Vertical transmission

102   from mothers to infants at delivery has been proposed as a possible mechanism of neonatal CA-

103   MRSA acquisition (30, 37), and while it is clear that *S. aureus* and MRSA can colonize the

104   vaginal tract during pregnancy, essentially nothing is known about specific bacterial factors that

105   promote vaginal persistence.

106   In this study, we have adapted a murine model of vaginal colonization by Group B

107   *Streptococcus* (GBS) (38), to investigate MRSA vaginal colonization. We determined that

108   divergent MRSA strains, CA-MRSA USA300 and HA-MRSA252, can persist within the mouse

109   vaginal tract and that three mouse strains, CD-1, C57BL/6, and BALB/c, can be colonized with

110   MRSA. We detected fluorescent MRSA in the vaginal lumen as well as cervical and uterine

111   tissues of colonized mice and immunohistochemical staining showed an increase of neutrophils

112   in colonized mice compared to naïve mice. We found that a MRSA strain lacking fibrinogen-

113   binding surface adhesins was attenuated in both *in vitro* and *in vivo* models of vaginal

114   colonization. Lastly, RNA-sequencing analysis of bacteria growing *in vivo* revealed the

115   importance of iron homeostasis in promoting MRSA persistence within the mouse vagina.

116   Mutant USA300 strains lacking the siderophore transporter FhuCBG or the cell-surface heme

117   receptor IsdB were significantly attenuated in their ability to colonize the vaginal tract *in vivo*.

118

119   **RESULTS**

120   **MRSA colonization of the reproductive tract.**

121   To characterize the ability of MRSA to attach to epithelial cells of the lower female

122   reproductive tract, we performed quantitative adherence assays with community-associated

123   USA300 strain LAC (39) and hospital-acquired strain MRSA252 (40) as described in (41) and in

124   the Methods. An inoculum of 10^5 CFU/well (MOI = 1) was added to confluent monolayers of

125   immortalized human vaginal (VK2), ectocervical (Ect1), and endocervical (End1) epithelial

126   cells. Following a 30-minute incubation, the cells were washed to remove all nonadherent

127   bacteria. Data are expressed as percent recovered cell-associated MRSA relative to the initial

128   inoculum. Both strains exhibited substantial adherence to all three cell lines, ranging from 30-

129   57% of the original inoculum (Fig. 1A and B). Next, we assessed the ability of both MRSA

130   strains to initiate colonization of the murine vaginal tract. 8-week old female CD-1 mice were

131   treated with 17β-estradiol 1-day before inoculation with 10^7 CFU of either USA300 or

132   MRSA252. The next day the vaginal lumen was swabbed and then we euthanized the animals

133   and collected the vagina, cervix, and uterus from each mouse to quantify bacterial load. The total

134   CFU from the swab or tissue homogenates was determined by plating on *S. aureus* CHROMagar

135   supplemented with cefoxitin. Both strains of MRSA were recovered from the majority of mice 1-

136   day post-inoculation in all tissues, and the CFU recovered from the swab were similar to the total

137   CFU counts from the vaginal tissue homogenates (Fig. 1C and D). This level and range in

138   recovered CFU is similar to what we have observed using this mouse model for GBS

139   colonization (38). In a subsequent experiment, mice were inoculated with USA300 expressing a

140   fluorescent DsRed protein and we harvested the female reproductive tract 1-day post-

141   colonization for histological analysis. We made serial sections of these tissues and performed

142   H&E staining to examine overall tissue morphology (Fig 1E, G, and I) and fluorescent

143   microscopy to visualize USA300 (Fig 1F, H, J, K, and L).   We observed numerous red

144   fluorescent bacteria contained within the lumen of the vagina (red arrows) (Fig. 1F). We could

145   also see MRSA in the cervical and uterine lumen, as well as within the lamina propria of those

146   organs (green arrows) (Fig. 1H, J, K, and L)

147

148   **MRSA vaginal persistence and host response.**

149   To assess vaginal persistence, mice were colonized with USA300 or MRSA252 and

150   swabbed to determine bacterial load over time. We recovered similar CFU from mice colonized

151   with either MRSA strain and we observed that both strains exhibited similar persistence within

152   the mouse vagina. While all mice were initially highly colonized by both MRSA strains, some

153   remained highly colonized while MRSA was cleared from other mice. (Fig. 2A and B). We also

154   assessed USA300 vaginal colonization for multiple mouse strains and observed the highest mean

155   CFUs from BALB/c mice while C57BL/6 and CD-1 mice were colonized to a lower level (Fig.

156   S1). Furthermore, MRSA was cleared more rapidly from the vaginal tract of CD-1 mice and

157   persisted the longest in BALB/c mice (Fig. S1).

158   As we observed eventual clearance of MRSA from the vaginal tract, we examined the

159   presence of neutrophils in vaginal tissue of mice colonized with MRSA compared to naïve mice.

7

160   Previous studies have shown that neutrophils respond to vaginal colonization by pathogenic

161   *Streptococcus* species, namely GBS and *Streptococcus pyogenes* (Group A *Streptococcus*, GAS),

162   and that neutrophils contribute to host defense and ultimate bacterial clearance (42-44). To

163   visualize neutrophils during colonization by MRSA, we collected vaginal tissues from mice 1-

164   day and 3-days post-inoculation with USA300 and made serial sections for H&E staining and

165   labelling with an antibody against the neutrophil marker Gr-1. H&E analysis showed that there

166   were no obvious differences in morphology of the vaginal lumen between naïve and colonized

167   mice (Fig. 2C, E, G, I, K, and M). We observed very few Gr-1 positive cells in the tissue sections

168   form naïve mice (Fig. 2D and F). In contrast to those from naïve mice, the tissue sections from

169   mice colonized with USA300 for 1-day contained numerous neutrophils within the vaginal

170   lamina propria (Fig. 2H and J). At 3-days post-inoculation we detected neutrophils within the

171   vaginal lumen (Fig. 2L and N).

172

173   **Adherence to fibrinogen impacts MRSA vaginal colonization.**

174   In a previous study, we demonstrated that GBS Fg binding contributed to vaginal

175   persistence (45). Also, several studies have shown the importance of *S. aureus* interactions with

176   extracellular matrix components, including Fg, in colonization and disease progression (46-49).

177   USA300 binding to Fg is primarily mediated by the four sortase-anchored surface adhesins ClfA,

178   ClfB, FnbA, and FnbB. (8, 46, 50). The serine-aspartate adhesins SdrC, SdrD, and SdrE are in

179   the same protein family as ClfA/B (51) and have been reported to bind nasal epithelia (23). To

180   eliminate these adherence functions, a USA300 strain was engineered where all of these adhesins

181   were deleted or disrupted by incorporating four separate mutations (Δ*clfA clfB*::Tn Δ*fnbAB*

182   *sdrCDE*::Tet; hereafter called "Fg adhesin mutant"). Compared to WT USA300, the Fg adhesin

183   mutant was significantly less adherent to Fg (Fig. 3A). Quantitative adherence assays showed

184   that the fibrinogen adhesin mutant exhibited decreased attachment to VK2 vaginal epithelial cells

185   (Fig. 3B), and we could visualize this difference via Gram staining (Fig. 3C and D). Further, the

186   Fg adhesin mutant was also less adherent to Ect1 and End1 cervical epithelial cells (Fig. 3E and

187   F). To assess the impact of these important surface adhesins during *in vivo* colonization, we co-

188   challenged mice with both WT USA300 and the Fg adhesin mutant. Initially we recovered

189   similar CFUs of both strains from the mice. However, by 3-days post-inoculation, mice were

190   significantly less colonized by the Fg adhesin mutant compared to WT USA300 (Fig. 3G). At 5-

191   days post-inoculation, we could recover WT USA300 CFU from 60% of the mice while only

192   30% were still colonized by the Fg adhesin mutant (Fig. 3G).

193

194   **Transcriptome analysis during MRSA vaginal colonization**

195   Although the Fg adhesin mutant was impaired in vaginal persistence compared to WT

196   USA300, we did not observe a significant difference in recovered CFUs between the two strains

197   during the first two days of colonization, and a few mice remained colonized with the Fg adhesin

198   mutant at later time points (Fig. 1G). Thus, we hypothesized that other bacterial factors are

199   involved in promoting MRSA vaginal carriage. To determine the impact of vaginal colonization

200   on MRSA gene expression, we performed transcriptome analysis by RNA-sequencing of

201   USA300 recovered from the mouse vagina compared to USA300 cultured under laboratory

202   conditions. For these experiments, we utilized the CD-1 mouse strain as likely in this background

203   the bacteria encounter more host pressure to maintain colonization. Mice were pre-treated with

204   17β-Estradiol, inoculated with 10^7 CFU of USA300, and swabbed at 5hrs, 1-day, and 3-days

205   post-inoculation for RNA isolation. The same mice were swabbed 2-, 4-, 6-, and 8-days post-

206   inoculation for CFU enumeration (Fig. 4A and B). Based on swab CFU counts, we selected

207   samples from 18 mice (purple circles) for RNA-sequencing analysis (Fig. 4B). RNA samples

208   from 6 mouse swabs were pooled to generate 3 replicates for each time-point to compare to

209   triplicate culture samples. Principle component analysis (PCA) for all of the samples showed that

210   culture samples clustered separately from mouse samples (Fig. 4C). Next, we compared mouse

211   samples from each time point to the culture samples and observed 709 genes were significantly

212   down-regulated (Fig. 4D) and 741 genes were significantly upregulated (Fig. 4E) in the mouse

213   (Table. S1.) Volcano plots of the $\log_2$(fold change) vs. $-\log_{10}$(P value) show that many of the

214   differentially upregulated and downregulated changes were highly significant at all three time

215   points compared to culture (Fig. 4F-H). We observed significant overlap in differentially

216   expressed transcripts at the various time points; over half of the differentially upregulated and

217   downregulated genes were the same at all three time points (Fig. 4E).

218   We identified genes encoding transcriptional regulators, toxins, extracellular enzymes,

219   and extracellular matrix-binding surface proteins that were significantly upregulated at all three

220   time points (Table 1). Interestingly, while only one immune evasion factor, chemotaxis inhibitor

221   (*chs*), was upregulated at all three time points, additional immune evasion genes were

222   significantly upregulated at 3-days post-inoculation. We observed a similar trend with genes

223   encoding components of the type VII secretion system (T7SS), which has been shown to

224   contribute to *S. aureus* virulence and competition with other microbes in polymicrobial settings

225   (52, 53). At 5 hrs post-inoculation, only 5 T7SS genes were significantly upregulated while 14

226   genes were upregulated at 1-day and 3-days post-inoculation (Table 1).

227

228   **Iron homeostasis impacts vaginal persistence.**

229   Though there were global transcriptional changes, the most highly-significant,

230   differentially-expressed transcripts belonged to iron uptake and export systems. The most highly

231   induced was the iron-surface determinant *isd* heme acquisition system (*isdBACDEFG* and *srtB).*

232   Other genes included those involved in the production of the siderophore staphyloferrin B (SB)

233   (*sbnABCDEFGHI*) as well as its importer (*sirAB*), the staphyloferrin A (SA) importer (*htsABC*),

234   the xeno-siderophore transporter (*fhuCB*), as well as the catechol/catecholamine iron transporter

235   system (*sstABCD*). Lastly, the heme-regulated export *hrt* system, was highly down-regulated

236   during colonization (*hrtAB*). (Fig. 5A) (54-57). As these results strongly suggest that the vaginal

237   environment is iron limited, we performed inductively coupled plasma mass spectrometry (ICP-

238   MS) to determine the iron concentration in vaginal lavage fluid from naïve mice and mice

239   colonized with USA300. We observed a very low concentration of iron (0.52 μM), irrespective

240   of MRSA colonization, compared to the level present in tryptic soy broth (TSB) (10 μM) (Fig.

241   5B).

242   To confirm the differential expression of iron-uptake systems by USA300, we incubated

243   USA300 in mouse vaginal lavage fluid and performed RT-qPCR to compare transcripts of select

244   iron-homeostasis genes between bacteria grown in lavage fluid and bacteria cultured under

245   laboratory conditions in TSB. Similar to our RNA-seq results, the RT-qPCR analysis revealed an

246   increase in *sirB*, *sbnA*, *isdB*, *isdD*, *srtB*, *htsC*, and *htsB* transcripts in MRSA cultured in vaginal

247   lavage fluid (Fig. 5C to 5I). Additionally, *hrtA* and *hrtB* were significantly downregulated in

248   MRSA from vaginal lavage compared to MRSA grown in TSB (Fig. 5J and 5K).

249   To assess the impact of iron uptake by MRSA on vaginal persistence, we co-colonized

250   mice with WT USA300 and either Δ*fhuCBG* or *isdB*::Tn mutants. In addition to its role in the

251   uptake of xeno-siderophores, the FhuC ATP-ase also provides energy needed for uptake of the

252   siderophores staphyloferrin A and staphyloferrin B. Therefore, the Δ*fhuCBG* mutant is defective

253   in the transport of all siderophores (58). Also, our RNA-seq results show that at all three time

254   points, the most highly upregulated gene was *isdB*, which encodes the hemoglobin-binding

255   surface protein that transports heme to downstream components of the *isd* system (55). *isdB*

256   transcripts from mouse samples were increased 210-fold at 5hrs, 90-fold at 1-day, and 117-fold

257   at 3-days post-inoculation compared to culture (Table S1 and Fig. 5A). Compared to WT

258   USA300, the Δ*fhuCBG* mutant and the *isdB*::Tn mutant were cleared significantly faster from

259   the mouse vagina (Fig. 5L and M). Because a previous study reported that IsdB may impact

260   bacterial attachment to host cells (59), we quantified adherence of the *isdB*::Tn mutant to VK2,

261   Ect1, and End1 cells *in vitro* and observed no defect compared to WT USA300 (Fig. S2).

262

263   **DISCUSSION**

264   *S. aureus* is capable of causing disease at nearly every site of the body (60), and MRSA

265   colonization of the skin as well as mucosal sites, such as the nares and the vaginal tract, is a

266   necessary initial step preceding the development of invasive disease (27, 37, 61-63). While many

267   studies have investigated host and bacterial determinants of *S. aureus* colonization of the skin

268   and nares as well as subsequent infection, little is known about factors which influence vaginal

269   niche establishment and persistence. Because vaginal carriage during pregnancy represents a

270   major risk factor for transmission of this pathogen to the newborn (24, 25, 64, 65), we utilized *in*

271   *vitro* and *in vivo* models of MRSA vaginal colonization to identify determinants of persistence

272   within the female reproductive tract. The results of our study reveal that MRSA can interact

273   directly with the female reproductive tract epithelium *in vitro* and *in vivo*, and that the expression

274   of cell-wall anchored Fg binding adhesins as well as iron-acquisition systems promote MRSA

275   vaginal colonization.

276   The effect of *S. aureus* colonization on the host immune response has been well-

277   characterized at many epithelial sites. *S. aureus* on the skin promotes a robust inflammatory

278   response involving both the innate and adaptive immune system (66, 67). Neutrophils in

279   particular are rapidly and highly recruited to the site of *S. aureus* skin infection and are key

280   mediators of clearance of the pathogen (68-75). Our studies on GBS vaginal carriage have shown

281   a clear role for neutrophils in combatting GBS colonization of this host site (43, 76).

282   Additionally, neutrophils have been shown to respond to other common pathogens of the vaginal

283   tract such as the fungus *Candida albicans* (77, 78) and the Gram-negative bacterium *Neisseria*

284   *gonorrhoeae* (79). In this study, we observed an increased neutrophil presence in the vaginal

285   tissues from mice colonized by MRSA compared to naïve controls. Interestingly, while there is

286   obvious neutrophil infiltration of the lamina propria of the vagina 1-day post-colonization with

287   MRSA, we did not detect neutrophils in the vaginal lumen at this early time point. In contrast, at

288   3-days post-inoculation, we could visualize many neutrophils within the vaginal lumen. The

289   timing of the infiltration of neutrophils into the vaginal lumen coincides with the increased

290   expression of immune evasion factors by MRSA; in our RNA-sequencing analysis we observed

291   significant upregulation of these factors at 3-days post-inoculation and not at earlier time points.

292   Future studies aimed at further characterizing the dynamics of neutrophil response to MRSA in

293   the female reproductive tract and their extravasation into the vaginal lumen may reveal new

294   insights into host immune responses common to all vaginal pathogens as well as those specific to

295   MRSA.

13

296   The impact of *S. aureus* interactions with Fg on colonization and disease at various tissue

297   sites has been well-characterized. In the context of invasive infections, Fg and fibrin can promote

298   clearance of *S. aureus* by containing the bacteria within aggregates (80, 81). Additionally, Fg can

299   stimulate the production of inflammatory cytokines and activate neutrophils (82-84). However,

300   *S. aureus* has also been shown to target Fg to promote persistence and disease in the host. The

301   bacterium can interact with Fg in order to coagulate or to form clumps which help it evade

302   immune detection, and this clumping is mediated by surface Fg binding adhesins including ClfA,

303   ClfB (46, 85-88). There is also evidence that *S. aureus* can alter gene regulation in the presence

304   of fibrinogen-containing clumps to enhance expression of virulence determinants (89).

305   Moreover, *S. aureus* can use Fg as part of its biofilm structure to promote persistence within the

306   host (90). Our data suggest that, in the context of vaginal colonization, MRSA interactions with

307   Fg are necessary for persistence within the host. A mutant deficient in Fg binding was

308   significantly impaired in its ability to adhere to human female reproductive tract cells *in vitro*

309   and was also rapidly cleared from the vaginal tract *in vivo* compared to the WT. These results

310   hint that the benefits of MRSA binding to Fg outweigh the potential detriments for the pathogen

311   during vaginal colonization.

312   While a majority of mice rapidly clear the Fg adhesin mutant during vaginal colonization,

313   it is able to persist in some of the animals (Fig. 3G). This result suggests that there are likely

314   other factors that contribute to *in vivo* vaginal colonization. To identify additional determinants

315   of vaginal persistence, we performed RNA-sequencing to profile the transcriptome of MRSA

316   during vaginal colonization. We observed that over one-quarter of the genes of USA300 were

317   differentially expressed during *in vivo* colonization, and over half of those genes were

318   differentially expressed at all three *in vivo* time points that were analyzed. Of note, many of the

14

319   most highly and significantly differentially expressed genes belonged to iron-acquisition or iron-

320   homeostasis pathways. Our observation that genes involved in iron uptake were upregulated was

321   not surprising since their expression is controlled by iron levels and our ICP-MS data revealed

322   the vaginal environment to be limited in iron (Fig. 5B). Using our *in vivo* murine vaginal

323   colonization model, we confirmed that mutants in *fhuCBG* and *isdB* exhibited decreased

324   persistence compared to the isogenic WT MRSA strain. Numerous reports have demonstrated

325   the importance of nutrient iron for *S. aureus* growth and pathogenicity (55, 91, 92), and the

326   results of our study highlight the necessity of this metal for MRSA persistence within the vaginal

327   environment. That the Δ*fhuCBG* mutant was attenuated in this model was interesting because,

328   while FhuCBG is known to transport hydroxamate-type siderophores which *S. aureus* does not

329   synthesize (57, 93), FhuC is also the ATP-ase which provides energy for uptake of both SA and

330   SB siderophores (55, 58). Both WT and the Δ*fhuCBG* mutant should, under the iron-restricted

331   conditions during vaginal colonization, express SA and SB. Given that the Δ*fhuCBG* mutant

332   cannot transport these siderophores, the extracellular environment becomes more iron restricted

333   to the mutant as it cannot access SA-Fe and SB-Fe chelates.

334   The limitation of iron is a major host mechanism for defending against pathogens

335   because this metal is vital for bacterial growth and metabolic processes (55, 94, 95). Other

336   transcriptomic studies examining *S. aureus* growing *in vivo* during invasive infections have

337   shown that the bacteria respond to nutrient limitation within the host. One study which compared

338   the transcriptomes of *S. aureus* in a murine osteomyelitis model to bacteria grown under

339   laboratory conditions revealed the importance of iron homeostasis mechanisms, especially the

340   Isd pathway, during chronic infection (96). Another analysis of USA300 gene expression during

341   human and mouse infections also showed upregulation of iron transporters *in vivo* (97).

342   Interestingly, many reports have shown that neutrophils can play an active role in limiting iron in

343   numerous host sites, including the vagina, during exposure to a bacterial pathogen (98-101). The

344   precise mechanisms by which the host restricts iron availability during colonization warrants

345   further research as this would provide insight into the exact function of neutrophils in controlling

346   MRSA vaginal persistence.

347   We have developed a murine model of *S. aureus* vaginal colonization and this study is

348   the first to investigate the molecular mechanisms that promote vaginal carriage and persistence

349   by MRSA. This mouse model will be useful for continued studies on MRSA-host interactions

350   within a mucosal environment. Here we demonstrate the importance of Fg binding as well as

351   iron-acquisition in promoting long-term colonization. Additionally, we observed that neutrophils

352   respond to MRSA presence in the vagina and that the bacteria upregulate the expression of

353   immune-modulating genes during the course of colonization. Further investigation into these

354   specific colonization determinants could yield therapeutic interventions to treat MRSA

355   persistence within this host niche.

356

357   **MATERIALS AND METHODS**

358   **Bacterial strains and culture conditions.**

359   *S. aureus* strains USA300 (39) and MRSA252 (40) were used for the experiments. *S.*

360   *aureus* was grown in tryptic soy broth (TSB) at 37 ℃ and growth was monitored by measuring

361   the optical density at 600nm (OD_{600}). For selection of *S. aureus* mutants, TSA (tryptic soy agar)

362   was supplemented with chloramphenicol (Cm) (10 μg/mL), erythromycin (Erm) (3 μg/mL), or

363   tetracycline (Tet) (1 μg/mL).

16

364   To generate the Fg adhesin mutant, first the *fnbAB* operon was deleted using allelic

365   replacement. Phages 80α or 11 were used for transduction between *S. aureus* strains (102). The

366   *fnbAB* markerless deletion plasmid pHC94 was constructed using Gibson assembly with the

367   plasmid backbone coming from amplification of pJB38 (103) using primers pJB R2 and pJB38

368   F2. The region upstream of *fnbA* was amplified with primers fnbAB delA and fnbAB delB, and

369   the region downstream of *fnbB* was amplified using fnbAB delC and fnb delD (Table S2). The

370   resulting plasmid was electroporated in *S. aureus* RN4220 (104), selecting on TSA Cm plates at

371   30°C. The plasmid was then transduced into *S. aureus* strain LAC Δ*clfA* (85). Individual

372   colonies were streaked on TSA Cm plates incubated at 42°C to select for integration of the

373   plasmid into the chromosome. Single colonies were grown in TSB at 30°C and re-inoculated into

374   fresh media for several days before plating on TSA containing anhydrotetracycline (0.3 μg/mL)

375   to select for loss of the plasmid, creating the LAC Δ*clfA* Δ*fnbAB* mutant. The *clfB*::Tn mutation

376   was than transduced into this background from the Nebraska Transposon Mutant Library (105)

377   and selected on TSA Erm plates.

378   The *isdB mariner*-based transposon *bursa aurealis* mutation (JE2 *isdB*::ΦNΣ, NE1102)

379   from the Nebraska Transposon Library (105) into USA300 LAC with phage 11 as described

380   previously (106). *S. aureus* genomic DNA of LAC* *isdB*::ΦNΣ was isolated using Puregene

381   DNA purification kit (Qiagen) and the transposon insertion was verified by PCR with primers

382   KAS249 and KAS250 (Table S2) .

383   The *fhuCBG* mutant (58) and the DsRed expressing USA300 strain were generated

384   previously (107).

385

386   *In vitro* **MRSA adherence assays.**

387   Immortalized VK2 human vaginal epithelial cells, Ect1 human ectocevical endothelial

388   cells, and End1 human endocervical epithelial cells were obtained from the American Type

389   Culture Collection (VK2.E6E7, ATCC CRL-2616; Ect1/E6E7, ATCC CRL-2614; End1/E6E7,

390   ATCC CRL-2615) and were maintained in keratinocyte serum-free medium (KSFM; Gibco)

391   with 0.1 ng/mL human recombinant epidermal growth factor (EGF; Gibco) and 0.05 mg/ml

392   bovine pituitary extract (Gibco) at 37°C with 5% CO_2.

393   Assays to determine cell surface-adherent MRSA were performed as described

394   previously (41). Briefly, bacteria were grown to mid-log phase to infect cell monolayers

395   (multiplicity of infection [MOI] = 1). After a 30-min. incubation, cells were detached with 0.1

396   mL of 0.25% trypsin-EDTA solution and lysed with addition of 0.4 mL of 0.025% TritonX-100

397   by vigorous pipetting. The lysates were then serially diluted and plated on TSA to enumerate the

398   bacterial CFU. Experiments were performed at least three times with each condition in triplicate,

399   and results from a representative experiment are shown.

400   Crystal violet fibrinogen adhesion assays were performed as described in (85). Briefly,

401   96-well plates (Corning) were coated with 20 μg/mL of human fibrinogen and incubated with

402   100 μL of bacterial suspensions in PBS at OD_{600} = 1.0 for 1h at 37°C. Wells were then washed

403   and dried, and the adherent bacteria were stained with 0.1% crystal violet. The bound crystal

404   violet stain was solubilized with 33% acetic acid and measured at OD_{570}.

405   For Gram staining analysis, VK2 monolayers were grown in tissue culture treated

406   chamber slides (ThermoFisher) and infected with either WT USA300 or the fibrinogen adhesin

407   mutant at an MOI of 20. Following a 30 min incubation, the cell monolayers were washed to

408   remove any non-adherent bacteria then fixed with 10% formalin (Fisher) and Gram stained

409   (Sigma).

410

411   **Murine vaginal colonization model.**

412   Animal experiments were approved by the Institutional Animal Care and Use Committee

413   at the University of Colorado-Anschutz Medical Campus protocol #00316 and performed using

414   accepted veterinary standards. A mouse vaginal colonization model for GBS was adapted for our

415   studies (38). 8-week old female CD-1 (Charles River), C57BL/6 (Jackson), and BALB/c

416   (Jackson) mice were injected intraperitoneally with 0.5 mg 17β-estradiol (Sigma) 1 day prior to

417   colonization with MRSA. Mice were vaginally inoculated with 10^7 CFU of MRSA in 10μL PBS

418   and on subsequent days the vaginal lumen was swabbed with a sterile ultrafine swab (Puritan).

419   To assess tissue CFU, mice were euthanized according to approved veterinary protocols and the

420   female reproductive tract tissues were placed into 500μL PBS and bead beat for 2 min to

421   homogenize the tissues. The recovered MRSA was serially diluted and enumerated on

422   CHROMagar (Hardy Diagnostics) supplemented with 5.2 μg/mL of cefoxitin.

423

424   **Histology.**

425   Mouse female reproductive tract was harvested and embedded into OCT compound

426   (Sakura) and sectioned with a CM1950 freezing cryostat (Leica). For fluorescence microscopy,

427   coverslips were mounted with VECTASHIELD mounting medium with DAPI (Vector Labs).

428   H&E staining was performed using reagents from Sigma. Immunohistochemical analysis was

429   performed using a biotinylated primary antibody against Gr-1 (Biolegend), Streptavidin

19

430   conjugated to horse radish peroxidase (Jackson Immunoresearch), and AEC peroxidase substrate

431   kit (Vector Labs). Images were taken with a BZ-X710 microscope (Keyence).

432

433   **Generation of RNA-sequencing data.**

434   10^7 CFU of USA300 were inoculated into the mouse vagina and mice were swabbed

435   vaginally 5 hrs, 1-day, and 3-days post-inoculation for RNA recovery. Vaginal swabs were

436   placed into TRIzol reagent (Thermo Fisher), vortexed to dissociated bacteria from swabs, and

437   stored at -80°C. Swabs samples from 6 mice were pooled and bacteria were lysed by beating for

438   2 min at maximum speed on a bead beater (BioSpec Products). RNA was isolated by following

439   the manufacturer's protocol using a Direct-Zol RNA MiniPrep Plus kit (Zymo Research). For

440   each sample, 120 ng total RNA was ribodepleted using the Ribo-Zero Magenetic Gold Kit

441   (Epidemiology) from Epicentre (Illumina) following the manufacurer's protocol. Ribodeplete

442   RNA was then prepared into sequence libraries using the RNA Ultra II kit (New Enlgand

443   Biolabs) following the manufacturer's protocol without fragmentation. Libraries underwent 9

444   cycles of PCR efore 1X Ampure Bead purification (Beckman Coulter). Libraries were

445   quantified, pooled, and sequenced on an Illumina NextSeq500 with 75-base single reads

446   targeting 20M reads per samples.

447

448   **Analysis of RNA-sequencing data.**

449   Sequencing reads were aligned to the NCBI reference sequence with GenBank accession

450   number NC_007793.1 and expression levels were calculated using Geneious 11.1.5. Transcripts

451   with an adjusted P value < 0.05 and $\log_2$fold change ±1 were considered significantly

20

452   differentially expressed. PCA and volcano plots were generated using the ggplot2 package in R.

453   Venn diagrams were generated using the area-proportional Venn diagram tool (BioInfoRx).

454

455   **ICP-MS analysis**

456   Triplicate samples of mouse vaginal lavage and TSB samples were sent to the University

457   of Nebraska Spectroscopy and Biophysics Core. Fe56 and Fe57 isotope measurements were

458   combined to show total iron levels.

459

460   **RT-qPCR confirmation of RNA-sequencing.**

461   Vaginal lavage fluid was collected as described in (38) and filtered through 0.22µm Spin-

462   X centrifuge tube filters (Costar) to remove contaminants. Triplicated log phase cultures of

463   USA300 were pelleted and resuspended in filtered lavage fluid. Following a 2-hour incubation at

464   37°C, bacteria were collected by centrifugation and resuspended in Trizol, lysed by bead beating,

465   and RNA was isolated using the Direct-Zol RNA MiniPrep Plus kit as described above. RNA

466   was treated with Turbo DNase (Invitrogen) to remove contaminating DNA. cDNA was

467   generated using the Quanta cDNA synthesis kit (Quanta Biosciences) and qPCR was performed

468   using PerfeCTa SYBR Green reagent (Quanta) and a CFX96 Real-Time PCR thermal cycler

469   (Bio-rad). Fold changes were calculated using the Livak method (108).

470

471   **Data analysis.**

472   GraphPad Prism version 7.0 was used for statistical analysis and statistical significance

473   was accepted at P values of < 0.05 (* $P < 0.05$; ** $P < 0.00005$; *** $P < 0.0005$; **** $P <$

474   0.00005). Specific tests are indicated in figure legends.

475

483

484   **FIGURE LEGENDS**

485   **Figure 1. Modeling MRSA vaginal colonization.** (A and B) Adherence of USA300 (A) and

486   MRSA252 (B) to human vaginal (VK2), ectocervical (Ect1), and endocervical (End1)

487   endothelial cells. (C and D) CFU counts from vaginal swabs, vagina, cervix, and uterus

488   recovered 1-day post-inoculation with USA300 (C) or MRSA252 (D). Lines represent median

489   CFU. (E-L) Mice were colonized with DsRed expressing USA300. 1-day post-inoculation, the

490   female reproductive tract was harvested and 6μm sections of the vagina (E and F), cervix (G, H,

491   and K), and uterus (I, J, and L) were either stained with H&E (E, G, I) or labelled with DAPI and

492   imaged with an epifluorescent microscope to visualize nuclei and USA300 (F, H, J, K, and L).

493   The areas highlighted in (H) and (J) are expanded in (K) and (L). USA300 in the lumen of

494   tissues are indicated with red arrows, and USA300 within the lamina propia are indicated with

495   green arrows. Scale bar in (E) is 100μm.

496

497 **Figure 2. MRSA vaginal persistence and host response.** (A and B) USA300 and MRSA252

498 persistence within the CD-1 mouse vaginal tract. CFU counts for individual mice (A) and mean

499 recovered CFU from vaginal swabs (B) were monitored for 14 days. Lines in (A) represent

500 median CFU. (C-N) Histology of the mouse vagina during MRSA colonization. Mice were pre-

501 treated with 17β-estradiol and either remained naïve (C-F) or were inoculated with 10^7 CFU of

502 USA300 (G-N). 6μm serial sections were stained with H&E (C, E, G, I, K, M) or labelled with

503 an antibody against Gr-1 (D, F, H, J, L, N). Scale bar in (C) is 100μm.

504

505 **Figure 3. Adherence to fibrinogen impacts MRSA vaginal colonization.** (A) Adherence of

506 WT USA300 and the Fg adhesin mutant to Fg. (B-D) Adherence to VK2 cells. Monolayers of

507 VK2 cells were inoculated with WT USA300 or the Fg adhesin mutant for a quantitative

508 adherence assay (B) or Gram stains (C and D). Scale bar in (C) is 10 μm. (E and F) Adherence to

509 Ect1 (E) and End1 (F) epithelial cells. (G) WT USA300 and the Fg adhesin co-colonization.

510 Statistical analysis (A, B, E, and F) Unpaired t test. (G) Two-way ANOVA with Sidak's multiple

511 comparisons test. * P < 0.05; *** P < 0.0005; **** P < 0.00005.

512

513 **Figure 4. Transcriptome analysis during MRSA vaginal colonization.** (A) Experimental

514 design for RNA-sequencing analysis of mouse vaginal swabs. (B) CFU counts from mouse

515 vaginal swabs. Samples chosen for RNA-sequencing are highlighted in purple. (C) PCA plot for

516 triplicate samples of culture, 5hr, 1-day, and 3-days swabs. (D and E) Venn diagrams showing

517 genes expressed at significantly higher levels (fold change > 2, P value < 0.01) in culture (D) or

518 in mouse swab samples (E). (F-H) Volcano plots highlighting genes that are differentially

23

519   expressed in swab samples from 5hrs (F), 1-day (G), and 3-days (H) post-inoculation compared

520   to culture.

521

522   **Figure 5. Iron homeostasis impacts vaginal persistence.** (A) Differential expression of genes

523   in iron-acquisition and iron-export pathways. (B) ICP-MS analysis of vaginal lavage from naïve

524   and colonized mice, and TSB. (C-K) RT-qPCR confirmation of select RNA-sequencing iron-

525   homeostasis hits. (L) Co-colonization with WT USA300 and Δ*fhuCBG* mutant. (M) Co-

526   colonization with WT USA300 and *isdB*::Tn mutant. Statistical analysis: (B) One-way ANOVA.

527   (C-K) Unpaired t test. (L and M) Two-way ANOVA with Sidak's multiple comparisons test.

528

529   **Table 1. Virulence factors which were significantly upregulated during vaginal**

530   **colonization.** Genes which encode transcriptional regulators, toxins, secreted enzymes, and

531   ECM binding factors and were differentially expressed in mouse swab samples at all three time

532   points are listed with their respective fold changes relative to growth in TSB. Immune

533   modulation and T7SS genes which were not significantly differentially expressed at all time

534   points are indicated with asterisks.

535

536   **Supplemental Figure 1. USA300 vaginal colonization in different mouse strains.**

537   CD-1, C57BL/6, and BALB/c mice were inoculated with 10^7 CFU of USA300 and the percent of

538   mice colonized (A) as well as mean vaginal swab CFU (B) were monitored for 9 days.

539

540   **Supplemental Figure 2. WT USA300 and *isdB*::Tn adherence to (A) VK2, (B) End1, and**

541   **(C) Ect1 cells.**

542

Supplemental table 1. Differentially expressed genes in mouse swabs. All genes that were significantly differentially expressed in mouse samples are listed along with their adjusted P values, fold changes relative to culture in TSB, and absolute confidence.

546

Supplemental table 2. List of primers used in this study.

548

1. **Kluytmans J, van Belkum A, Verbrugh H.** 1997. Nasal carriage of Staphylococcus aureus: epidemiology, underlying mechanisms, and associated risks. Clin Microbiol Rev **10:**505-520.
2. **Chambers HF, Deleo FR.** 2009. Waves of resistance: Staphylococcus aureus in the antibiotic era. Nat Rev Microbiol **7:**629-641.
3. **DeLeo FR, Chambers HF.** 2009. Reemergence of antibiotic-resistant Staphylococcus aureus in the genomics era. J Clin Invest **119:**2464-2474.
4. **Lee BY, Singh A, David MZ, Bartsch SM, Slayton RB, Huang SS, Zimmer SM, Potter MA, Macal CM, Lauderdale DS, Miller LG, Daum RS.** 2013. The economic burden of community-associated methicillin-resistant Staphylococcus aureus (CA-MRSA). Clin Microbiol Infect **19:**528-536.
5. **David MZ, Daum RS.** 2010. Community-associated methicillin-resistant Staphylococcus aureus: epidemiology and clinical consequences of an emerging epidemic. Clin Microbiol Rev **23:**616-687.
6. **Kennedy AD, Otto M, Braughton KR, Whitney AR, Chen L, Mathema B, Mediavilla JR, Byrne KA, Parkins LD, Tenover FC, Kreiswirth BN, Musser JM, DeLeo FR.** 2008. Epidemic community-associated methicillin-resistant Staphylococcus aureus: recent clonal expansion and diversification. Proc Natl Acad Sci U S A **105:**1327-1332.
7. **Li M, Diep BA, Villaruz AE, Braughton KR, Jiang X, DeLeo FR, Chambers HF, Lu Y, Otto M.** 2009. Evolution of virulence in epidemic community-associated methicillin-resistant Staphylococcus aureus. Proc Natl Acad Sci U S A **106:**5883-5888.
8. **Foster TJ, Geoghegan JA, Ganesh VK, Hook M.** 2014. Adhesion, invasion and evasion: the many functions of the surface proteins of Staphylococcus aureus. Nat Rev Microbiol **12:**49-62.
9. **Pietrocola G, Nobile G, Rindi S, Speziale P.** 2017. Staphylococcus aureus Manipulates Innate Immunity through Own and Host-Expressed Proteases. Front Cell Infect Microbiol **7:**166.
10. **Seilie ES, Bubeck Wardenburg J.** 2017. Staphylococcus aureus pore-forming toxins: The interface of pathogen and host complexity. Semin Cell Dev Biol **72:**101-116.

578   11.   **Bretl DJ, Elfessi A, Watkins H, Schwan WR.** 2019. Regulation of the Staphylococcal
579   Superantigen-Like Protein 1 Gene of Community-Associated Methicillin-Resistant
580   Staphylococcus aureus in Murine Abscesses. Toxins (Basel) **11**.
581   12.   **Taglialegna A, Varela MC, Rosato RR, Rosato AE.** 2019. VraSR and Virulence Trait
582   Modulation during Daptomycin Resistance in Methicillin-Resistant Staphylococcus
583   aureus Infection. mSphere **4**.
584   13.   **Jenul C, Horswill AR.** 2018. Regulation of Staphylococcus aureus Virulence. Microbiol
585   Spectr **6**.
586   14.   **Wertheim HF, Vos MC, Ott A, van Belkum A, Voss A, Kluytmans JA, van Keulen PH,**
587   **Vandenbroucke-Grauls CM, Meester MH, Verbrugh HA.** 2004. Risk and outcome of
588   nosocomial Staphylococcus aureus bacteraemia in nasal carriers versus non-carriers.
589   Lancet **364:**703-705.
590   15.   **Cole AM, Tahk S, Oren A, Yoshioka D, Kim YH, Park A, Ganz T.** 2001. Determinants of
591   Staphylococcus aureus nasal carriage. Clin Diagn Lab Immunol **8:**1064-1069.
592   16.   **Peacock SJ, de Silva I, Lowy FD.** 2001. What determines nasal carriage of
593   Staphylococcus aureus? Trends Microbiol **9:**605-610.
594   17.   **O'Brien LM, Walsh EJ, Massey RC, Peacock SJ, Foster TJ.** 2002. Staphylococcus aureus
595   clumping factor B (ClfB) promotes adherence to human type I cytokeratin 10:
596   implications for nasal colonization. Cell Microbiol **4:**759-770.
597   18.   **Clarke SR, Brummell KJ, Horsburgh MJ, McDowell PW, Mohamad SA, Stapleton MR,**
598   **Acevedo J, Read RC, Day NP, Peacock SJ, Mond JJ, Kokai-Kun JF, Foster SJ.** 2006.
599   Identification of in vivo-expressed antigens of Staphylococcus aureus and their use in
600   vaccinations for protection against nasal carriage. J Infect Dis **193:**1098-1108.
601   19.   **Schaffer AC, Solinga RM, Cocchiaro J, Portoles M, Kiser KB, Risley A, Randall SM,**
602   **Valtulina V, Speziale P, Walsh E, Foster T, Lee JC.** 2006. Immunization with
603   Staphylococcus aureus clumping factor B, a major determinant in nasal carriage,
604   reduces nasal colonization in a murine model. Infect Immun **74:**2145-2153.
605   20.   **Wertheim HF, Walsh E, Choudhurry R, Melles DC, Boelens HA, Miajlovic H, Verbrugh**
606   **HA, Foster T, van Belkum A.** 2008. Key role for clumping factor B in Staphylococcus
607   aureus nasal colonization of humans. PLoS Med **5:**e17.
608   21.   **Ponnuraj K, Bowden MG, Davis S, Gurusiddappa S, Moore D, Choe D, Xu Y, Hook M,**
609   **Narayana SV.** 2003. A "dock, lock, and latch" structural model for a staphylococcal
610   adhesin binding to fibrinogen. Cell **115:**217-228.
611   22.   **Bowden MG, Heuck AP, Ponnuraj K, Kolosova E, Choe D, Gurusiddappa S, Narayana**
612   **SV, Johnson AE, Hook M.** 2008. Evidence for the "dock, lock, and latch" ligand binding
613   mechanism of the staphylococcal microbial surface component recognizing adhesive
614   matrix molecules (MSCRAMM) SdrG. J Biol Chem **283:**638-647.
615   23.   **Corrigan RM, Miajlovic H, Foster TJ.** 2009. Surface proteins that promote adherence of
616   Staphylococcus aureus to human desquamated nasal epithelial cells. BMC Microbiol
617   **9:**22.
618   24.   **Andrews WW, Schelonka R, Waites K, Stamm A, Cliver SP, Moser S.** 2008. Genital tract
619   methicillin-resistant Staphylococcus aureus: risk of vertical transmission in pregnant
620   women. Obstet Gynecol **111:**113-118.

25. **Beigi R, Hanrahan J.** 2007. Staphylococcus aureus and MRSA colonization rates among gravidas admitted to labor and delivery: a pilot study. Infect Dis Obstet Gynecol **2007:**70876.

26. **Chen KT, Huard RC, Della-Latta P, Saiman L.** 2006. Prevalence of methicillin-sensitive and methicillin-resistant Staphylococcus aureus in pregnant women. Obstet Gynecol **108:**482-487.

27. **Creech CB, Litzner B, Talbot TR, Schaffner W.** 2010. Frequency of detection of methicillin-resistant Staphylococcus aureus from rectovaginal swabs in pregnant women. Am J Infect Control **38:**72-74.

28. **Dancer SJ, Noble WC.** 1991. Nasal, axillary, and perineal carriage of Staphylococcus aureus among women: identification of strains producing epidermolytic toxin. J Clin Pathol **44:**681-684.

29. **Reiss-Mandel A, Rubin C, Maayan-Mezger A, Novikov I, Jaber H, Dolitzky M, Freedman L, Rahav G, Regev-Yochay G.** 2019. Patterns and Predictors of Staphylococcus aureus Carriage during the First Year of Life: a Longitudinal Study. J Clin Microbiol **57**.

30. **Lin J, Yao Z.** 2018. Maternal-Infant Correlation of Multidrug-Resistant Staphylococcus aureus Carriage: A Prospective Cohort Study. Front Pediatr **6:**384.

31. **Bratu S, Eramo A, Kopec R, Coughlin E, Ghitan M, Yost R, Chapnick EK, Landman D, Quale J.** 2005. Community-associated methicillin-resistant Staphylococcus aureus in hospital nursery and maternity units. Emerg Infect Dis **11:**808-813.

32. **Laibl VR, Sheffield JS, Roberts S, McIntire DD, Trevino S, Wendel GD, Jr.** 2005. Clinical presentation of community-acquired methicillin-resistant Staphylococcus aureus in pregnancy. Obstet Gynecol **106:**461-465.

33. **Nambiar S, Herwaldt LA, Singh N.** 2003. Outbreak of invasive disease caused by methicillin-resistant Staphylococcus aureus in neonates and prevalence in the neonatal intensive care unit. Pediatr Crit Care Med **4:**220-226.

34. **Saiman L, Cronquist A, Wu F, Zhou J, Rubenstein D, Eisner W, Kreiswirth BN, Della-Latta P.** 2003. An outbreak of methicillin-resistant Staphylococcus aureus in a neonatal intensive care unit. Infect Control Hosp Epidemiol **24:**317-321.

35. **Seybold U, Halvosa JS, White N, Voris V, Ray SM, Blumberg HM.** 2008. Emergence of and risk factors for methicillin-resistant Staphylococcus aureus of community origin in intensive care nurseries. Pediatrics **122:**1039-1046.

36. **Stafford I, Hernandez J, Laibl V, Sheffield J, Roberts S, Wendel G, Jr.** 2008. Community-acquired methicillin-resistant Staphylococcus aureus among patients with puerperal mastitis requiring hospitalization. Obstet Gynecol **112:**533-537.

37. **Top KA, Huard RC, Fox Z, Wu F, Whittier S, Della-Latta P, Saiman L, Ratner AJ.** 2010. Trends in methicillin-resistant Staphylococcus aureus anovaginal colonization in pregnant women in 2005 versus 2009. J Clin Microbiol **48:**3675-3680.

38. **Patras KA, Doran KS.** 2016. A Murine Model of Group B Streptococcus Vaginal Colonization. J Vis Exp doi:10.3791/54708.

39. **Boles BR, Thoendel M, Roth AJ, Horswill AR.** 2010. Identification of genes involved in polysaccharide-independent Staphylococcus aureus biofilm formation. PLoS One **5:**e10146.
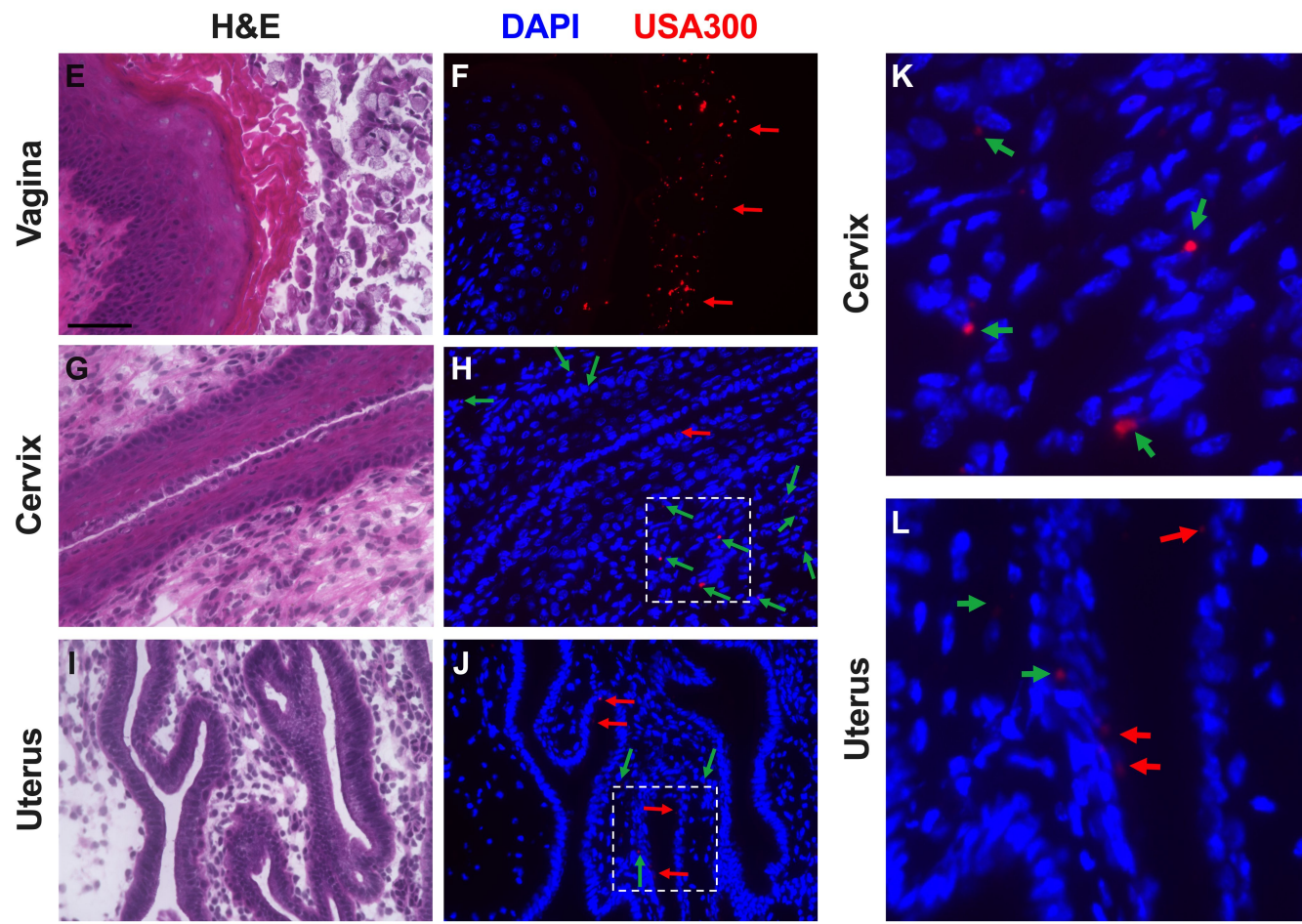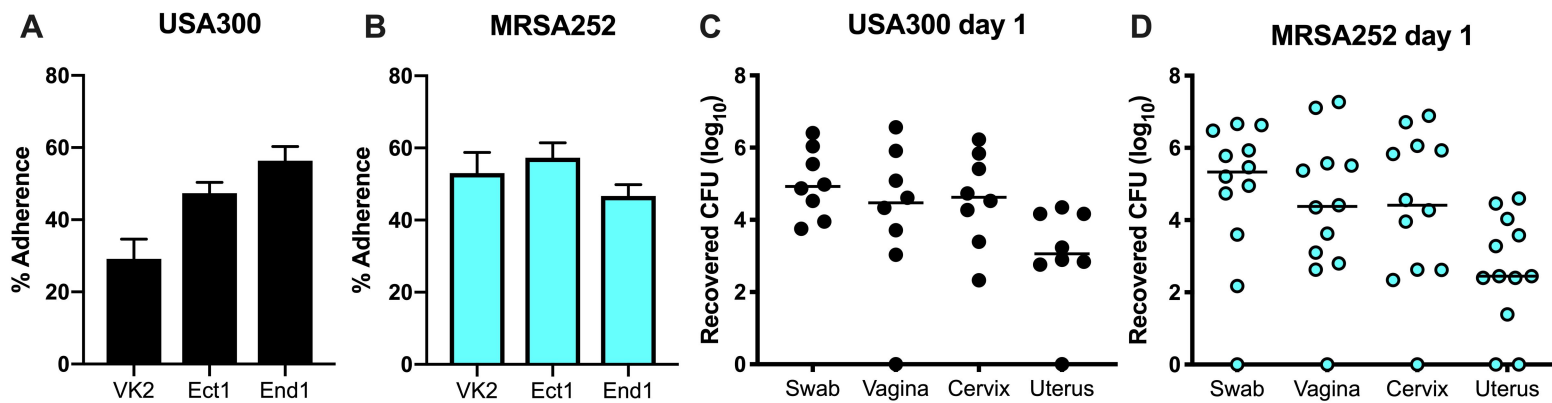
664   40.   **Holden MT, Feil EJ, Lindsay JA, Peacock SJ, Day NP, Enright MC, Foster TJ, Moore CE,**
665   **Hurst L, Atkin R, Barron A, Bason N, Bentley SD, Chillingworth C, Chillingworth T,**
666   **Churcher C, Clark L, Corton C, Cronin A, Doggett J, Dowd L, Feltwell T, Hance Z, Harris**
667   **B, Hauser H, Holroyd S, Jagels K, James KD, Lennard N, Line A, Mayes R, Moule S,**
668   **Mungall K, Ormond D, Quail MA, Rabbinowitsch E, Rutherford K, Sanders M, Sharp S,**
669   **Simmonds M, Stevens K, Whitehead S, Barrell BG, Spratt BG, Parkhill J.** 2004. Complete
670   genomes of two clinical Staphylococcus aureus strains: evidence for the rapid evolution
671   of virulence and drug resistance. Proc Natl Acad Sci U S A **101:**9786-9791.
672   41.   **Deng L, Mu R, Weston TA, Spencer BL, Liles RP, Doran KS.** 2018. Characterization of a
673   Two-Component System Transcriptional Regulator, LtdR, That Impacts Group B
674   Streptococcal Colonization and Disease. Infect Immun **86**.
675   42.   **Patras KA, Rosler B, Thoman ML, Doran KS.** 2015. Characterization of host immunity
676   during persistent vaginal colonization by Group B Streptococcus. Mucosal Immunol
677   **8:**1339-1348.
678   43.   **Patras KA, Wang NY, Fletcher EM, Cavaco CK, Jimenez A, Garg M, Fierer J, Sheen TR,**
679   **Rajagopal L, Doran KS.** 2013. Group B Streptococcus CovR regulation modulates host
680   immune signalling pathways to promote vaginal colonization. Cell Microbiol **15:**1154-
681   1167.
682   44.   **Carey AJ, Weinberg JB, Dawid SR, Venturini C, Lam AK, Nizet V, Caparon MG, Walker**
683   **MJ, Watson ME, Ulett GC.** 2016. Interleukin-17A Contributes to the Control of
684   Streptococcus pyogenes Colonization and Inflammation of the Female Genital Tract. Sci
685   Rep **6:**26836.
686   45.   **Wang NY, Patras KA, Seo HS, Cavaco CK, Rosler B, Neely MN, Sullam PM, Doran KS.**
687   2014. Group B streptococcal serine-rich repeat proteins promote interaction with
688   fibrinogen and vaginal colonization. J Infect Dis **210:**982-991.
689   46.   **Crosby HA, Kwiecinski J, Horswill AR.** 2016. Staphylococcus aureus Aggregation and
690   Coagulation Mechanisms, and Their Function in Host-Pathogen Interactions. Adv Appl
691   Microbiol **96:**1-41.
692   47.   **Rhem MN, Lech EM, Patti JM, McDevitt D, Hook M, Jones DB, Wilhelmus KR.** 2000. The
693   collagen-binding adhesin is a virulence factor in Staphylococcus aureus keratitis. Infect
694   Immun **68:**3776-3779.
695   48.   **Josse J, Laurent F, Diot A.** 2017. Staphylococcal Adhesion and Host Cell Invasion:
696   Fibronectin-Binding and Other Mechanisms. Front Microbiol **8:**2433.
697   49.   **Kwiecinski J, Jin T, Josefsson E.** 2014. Surface proteins of Staphylococcus aureus play an
698   important role in experimental skin infection. APMIS **122:**1240-1250.
699   50.   **Foster TJ, Hook M.** 1998. Surface protein adhesins of Staphylococcus aureus. Trends
700   Microbiol **6:**484-488.
701   51.   **Clarke SR, Foster SJ.** 2006. Surface adhesins of Staphylococcus aureus. Adv Microb
702   Physiol **51:**187-224.
703   52.   **Unnikrishnan M, Constantinidou C, Palmer T, Pallen MJ.** 2017. The Enigmatic Esx
704   Proteins: Looking Beyond Mycobacteria. Trends Microbiol **25:**192-204.
705   53.   **Cao Z, Casabona MG, Kneuper H, Chalmers JD, Palmer T.** 2016. The type VII secretion
706   system of Staphylococcus aureus secretes a nuclease toxin that targets competitor
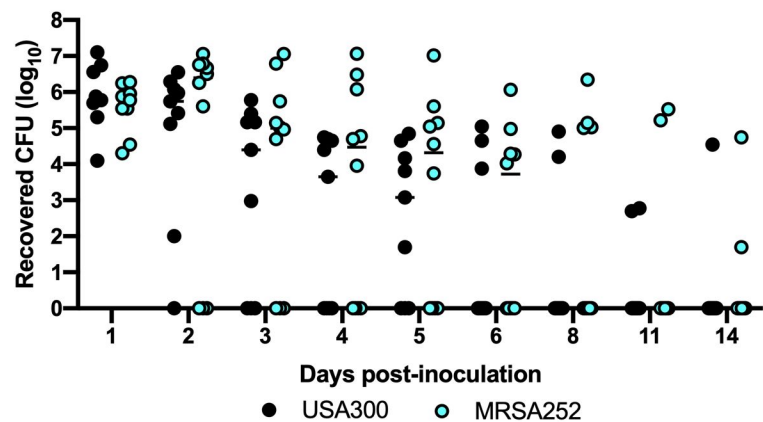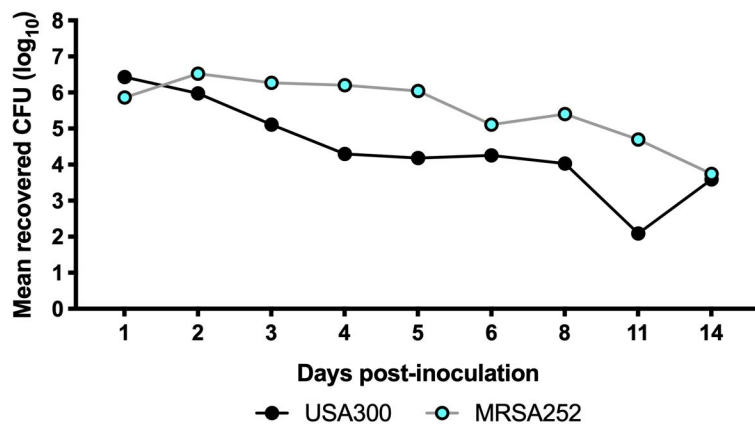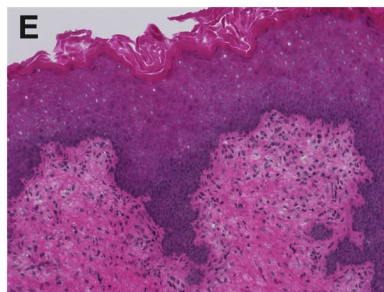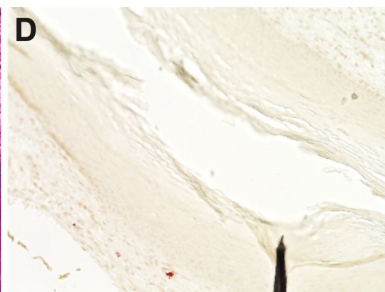707   bacteria. Nat Microbiol **2:**16183.
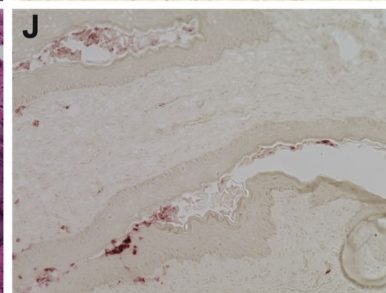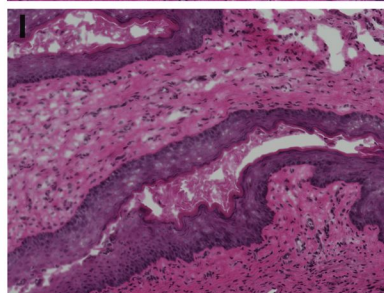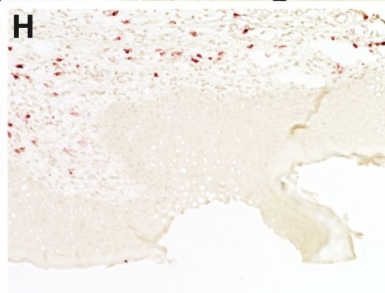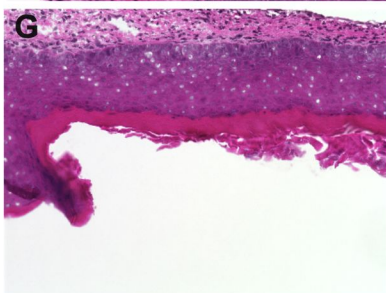
28

708   54.   **Beasley FC, Marolda CL, Cheung J, Buac S, Heinrichs DE.** 2011. Staphylococcus aureus
709   transporters Hts, Sir, and Sst capture iron liberated from human transferrin by
710   Staphyloferrin A, Staphyloferrin B, and catecholamine stress hormones, respectively,
711   and contribute to virulence. Infect Immun **79:**2345-2355.
712   55.   **Hammer ND, Skaar EP.** 2011. Molecular mechanisms of Staphylococcus aureus iron
713   acquisition. Annu Rev Microbiol **65:**129-147.
714   56.   **Stauff DL, Skaar EP.** 2009. The heme sensor system of Staphylococcus aureus. Contrib
715   Microbiol **16:**120-135.
716   57.   **Sheldon JR, Heinrichs DE.** 2015. Recent developments in understanding the iron
717   acquisition strategies of gram positive pathogens. FEMS Microbiol Rev **39:**592-630.
718   58.   **Speziali CD, Dale SE, Henderson JA, Vines ED, Heinrichs DE.** 2006. Requirement of
719   Staphylococcus aureus ATP-binding cassette-ATPase FhuC for iron-restricted growth and
720   evidence that it functions with more than one iron transporter. J Bacteriol **188:**2048-
721   2055.
722   59.   **Zapotoczna M, Jevnikar Z, Miajlovic H, Kos J, Foster TJ.** 2013. Iron-regulated surface
723   determinant B (IsdB) promotes Staphylococcus aureus adherence to and internalization
724   by non-phagocytic human cells. Cell Microbiol **15:**1026-1041.
725   60.   **Tong SY, Davis JS, Eichenberger E, Holland TL, Fowler VG, Jr.** 2015. Staphylococcus
726   aureus infections: epidemiology, pathophysiology, clinical manifestations, and
727   management. Clin Microbiol Rev **28:**603-661.
728   61.   **Wertheim HF, Melles DC, Vos MC, van Leeuwen W, van Belkum A, Verbrugh HA,**
729   **Nouwen JL.** 2005. The role of nasal carriage in Staphylococcus aureus infections. Lancet
730   Infect Dis **5:**751-762.
731   62.   **Coates R, Moran J, Horsburgh MJ.** 2014. Staphylococci: colonizers and pathogens of
732   human skin. Future Microbiol **9:**75-91.
733   63.   **Andrews JI, Fleener DK, Messer SA, Kroeger JS, Diekema DJ.** 2009. Screening for
734   Staphylococcus aureus carriage in pregnancy: usefulness of novel sampling and culture
735   strategies. Am J Obstet Gynecol **201:**396 e391-395.
736   64.   **Carey AJ, Duchon J, Della-Latta P, Saiman L.** 2010. The epidemiology of methicillin-
737   susceptible and methicillin-resistant Staphylococcus aureus in a neonatal intensive care
738   unit, 2000-2007. J Perinatol **30:**135-139.
739   65.   **Pinter DM, Mandel J, Hulten KG, Minkoff H, Tosi MF.** 2009. Maternal-infant perinatal
740   transmission of methicillin-resistant and methicillin-sensitive Staphylococcus aureus. Am
741   J Perinatol **26:**145-151.
742   66.   **Holtfreter S, Kolata J, Broker BM.** 2010. Towards the immune proteome of
743   Staphylococcus aureus - The anti-S. aureus antibody response. Int J Med Microbiol
744   **300:**176-192.
745   67.   **Krishna S, Miller LS.** 2012. Innate and adaptive immune responses against
746   Staphylococcus aureus skin infections. Semin Immunopathol **34:**261-280.
747   68.   **Segal AW.** 2005. How neutrophils kill microbes. Annu Rev Immunol **23:**197-223.
748   69.   **Kim MH, Granick JL, Kwok C, Walker NJ, Borjesson DL, Curry FR, Miller LS, Simon SI.**
749   2011. Neutrophil survival and c-kit(+)-progenitor proliferation in Staphylococcus aureus-
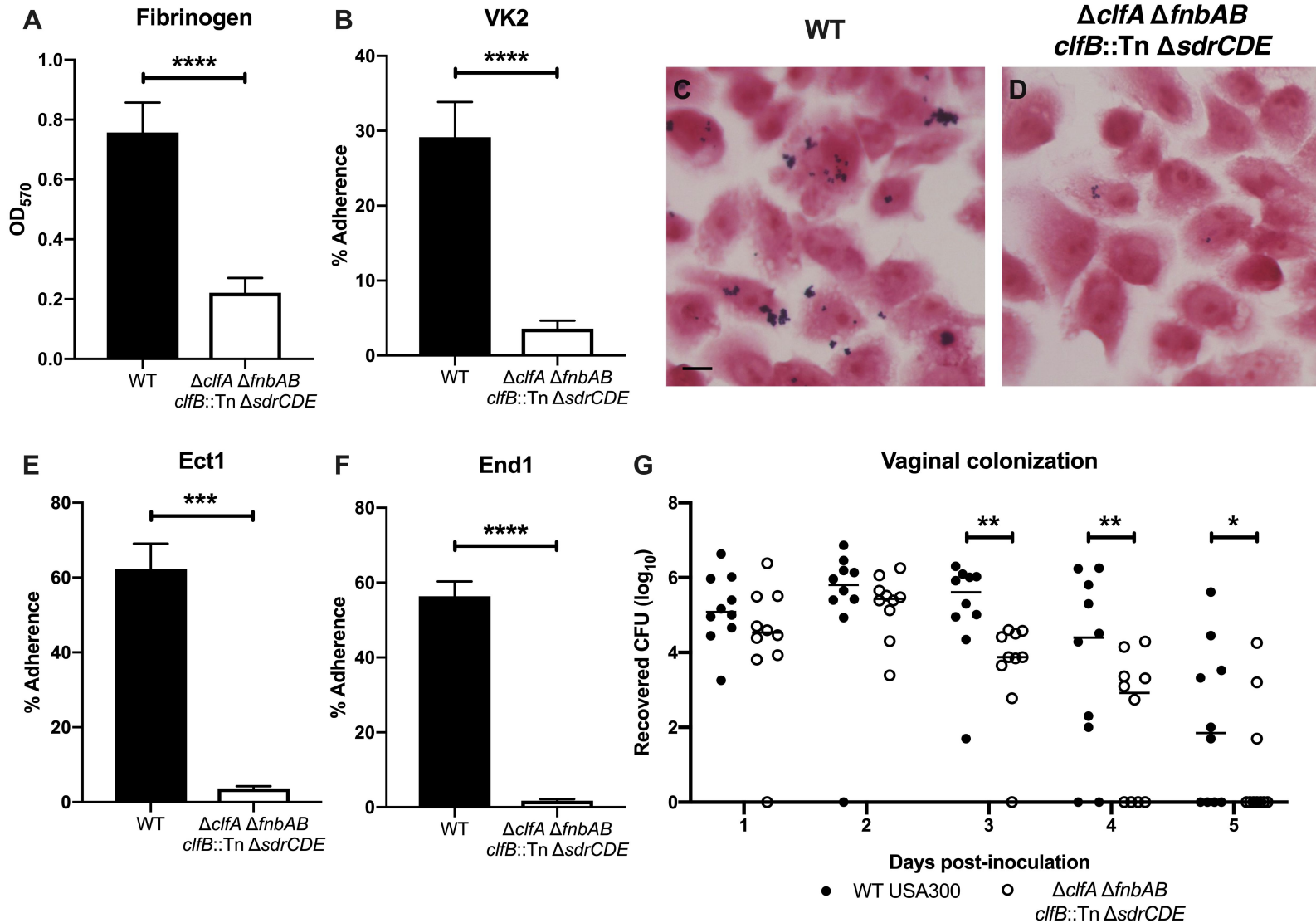750   infected skin wounds promote resolution. Blood **117:**3343-3352.

751 70. **Brinkmann V, Reichard U, Goosmann C, Fauler B, Uhlemann Y, Weiss DS, Weinrauch Y,**
752   **Zychlinsky A.** 2004. Neutrophil extracellular traps kill bacteria. Science **303:**1532-1535.

753 71. **Pilsczek FH, Salina D, Poon KK, Fahey C, Yipp BG, Sibley CD, Robbins SM, Green FH,**
754   **Surette MG, Sugai M, Bowden MG, Hussain M, Zhang K, Kubes P.** 2010. A novel
755   mechanism of rapid nuclear neutrophil extracellular trap formation in response to
756   Staphylococcus aureus. J Immunol **185:**7413-7425.

757 72. **Parlet CP, Kavanaugh JS, Crosby HA, Raja HA, El-Elimat T, Todd DA, Pearce CJ, Cech NB,**
758   **Oberlies NH, Horswill AR.** 2019. Apicidin Attenuates MRSA Virulence through Quorum-
759   Sensing Inhibition and Enhanced Host Defense. Cell Rep **27:**187-198 e186.

760 73. **Anderson LS, Reynolds MB, Rivara KR, Miller LS, Simon SI.** 2019. A Mouse Model to
761   Assess Innate Immune Response to Staphylococcus aureus Infection. J Vis Exp
762   doi:10.3791/59015.

763 74. **Miller LS, Simon SI.** 2018. Neutrophils in hot pursuit of MRSA in the lymph nodes. Proc
764   Natl Acad Sci U S A **115:**2272-2274.

765 75. **Molne L, Verdrengh M, Tarkowski A.** 2000. Role of neutrophil leukocytes in cutaneous
766   infection caused by Staphylococcus aureus. Infect Immun **68:**6162-6167.

767 76. **Carey AJ, Tan CK, Mirza S, Irving-Rodgers H, Webb RI, Lam A, Ulett GC.** 2014. Infection
768   and cellular defense dynamics in a novel 17beta-estradiol murine model of chronic
769   human group B streptococcus genital tract colonization reveal a role for hemolysin in
770   persistence and neutrophil accumulation. J Immunol **192:**1718-1731.

771 77. **Richardson JP, Willems HME, Moyes DL, Shoaie S, Barker KS, Tan SL, Palmer GE, Hube**
772   **B, Naglik JR, Peters BM.** 2018. Candidalysin Drives Epithelial Signaling, Neutrophil
773   Recruitment, and Immunopathology at the Vaginal Mucosa. Infect Immun **86**.

774 78. **Yano J, Noverr MC, Fidel PL, Jr.** 2017. Vaginal Heparan Sulfate Linked to Neutrophil
775   Dysfunction in the Acute Inflammatory Response Associated with Experimental
776   Vulvovaginal Candidiasis. MBio **8**.

777 79. **Soler-Garcia AA, Jerse AE.** 2007. Neisseria gonorrhoeae catalase is not required for
778   experimental genital tract infection despite the induction of a localized neutrophil
779   response. Infect Immun **75:**2225-2233.

780 80. **Dunn DL, Simmons RL.** 1982. Fibrin in peritonitis. III. The mechanism of bacterial
781   trapping by polymerizing fibrin. Surgery **92:**513-519.

782 81. **Kapral FA.** 1966. Clumping of Staphylococcus aureus in the peritoneal cavity of mice. J
783   Bacteriol **92:**1188-1195.

784 82. **Hsieh JY, Smith TD, Meli VS, Tran TN, Botvinick EL, Liu WF.** 2017. Differential regulation
785   of macrophage inflammatory activation by fibrin and fibrinogen. Acta Biomater **47:**14-
786   24.

787 83. **Rubel C, Fernandez GC, Dran G, Bompadre MB, Isturiz MA, Palermo MS.** 2001.
788   Fibrinogen promotes neutrophil activation and delays apoptosis. J Immunol **166:**2002-
789   2010.

790 84. **Rubel C, Fernandez GC, Rosa FA, Gomez S, Bompadre MB, Coso OA, Isturiz MA,**
791   **Palermo MS.** 2002. Soluble fibrinogen modulates neutrophil functionality through the
792   activation of an extracellular signal-regulated kinase-dependent pathway. J Immunol
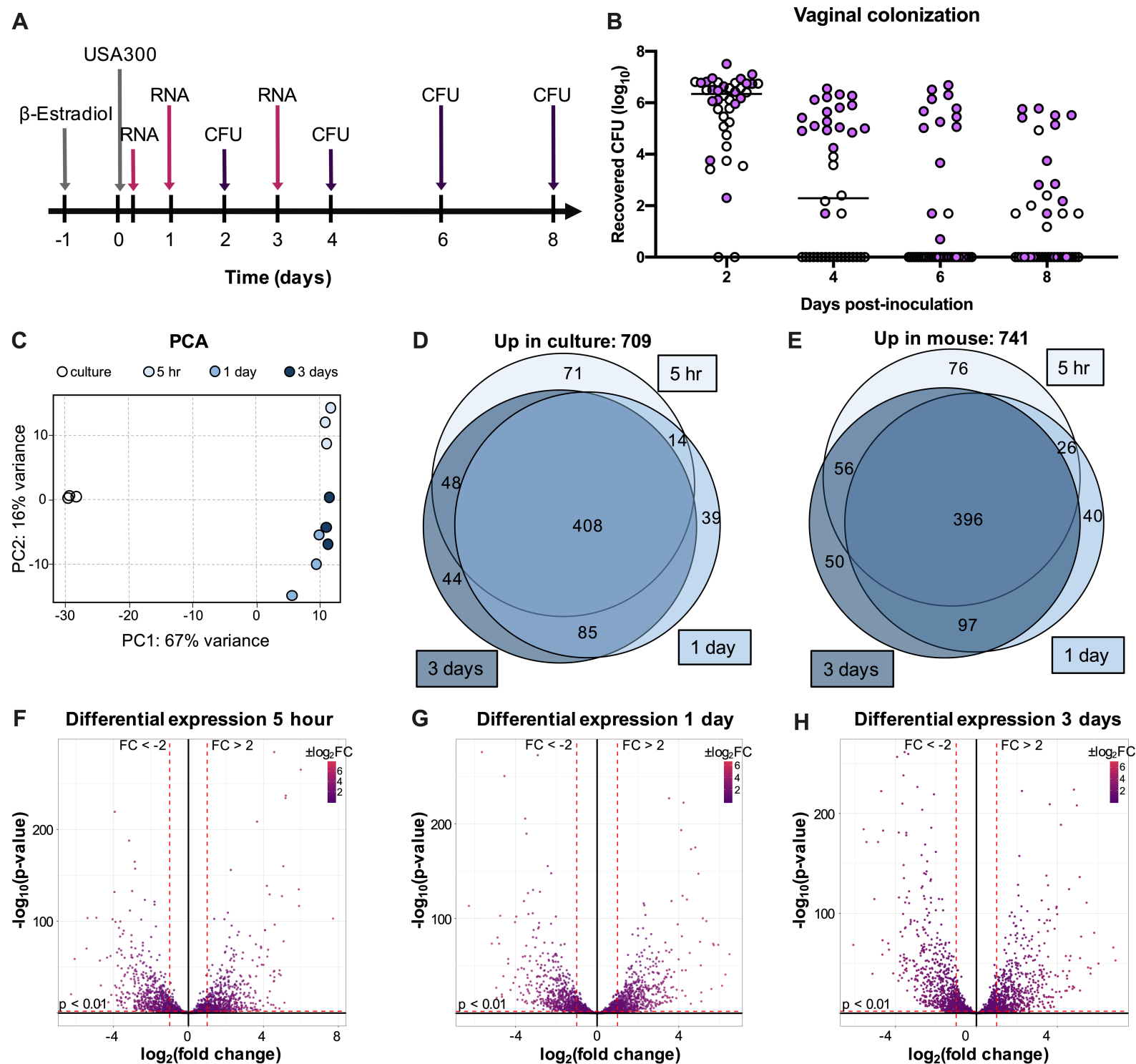793   **168:**3527-3535.

85. **Kwiecinski JM, Crosby HA, Valotteau C, Hippensteel JA, Nayak MK, Chauhan AK, Schmidt EP, Dufrene YF, Horswill AR.** 2019. Staphylococcus aureus adhesion in endovascular infections is controlled by the ArlRS-MgrA signaling cascade. PLoS Pathog **15:**e1007800.

86. **Walker JN, Crosby HA, Spaulding AR, Salgado-Pabon W, Malone CL, Rosenthal CB, Schlievert PM, Boyd JM, Horswill AR.** 2013. The Staphylococcus aureus ArlRS two-component system is a novel regulator of agglutination and pathogenesis. PLoS Pathog **9:**e1003819.

87. **Crosby HA, Schlievert PM, Merriman JA, King JM, Salgado-Pabon W, Horswill AR.** 2016. The Staphylococcus aureus Global Regulator MgrA Modulates Clumping and Virulence by Controlling Surface Protein Expression. PLoS Pathog **12:**e1005604.

88. **Cheng AG, McAdow M, Kim HK, Bae T, Missiakas DM, Schneewind O.** 2010. Contribution of coagulases towards Staphylococcus aureus disease and protective immunity. PLoS Pathog **6:**e1001036.

89. **Rothfork JM, Dessus-Babus S, Van Wamel WJ, Cheung AL, Gresham HD.** 2003. Fibrinogen depletion attenuates Staphyloccocus aureus infection by preventing density-dependent virulence gene up-regulation. J Immunol **171:**5389-5395.

90. **Kwiecinski J, Peetermans M, Liesenborghs L, Na M, Bjornsdottir H, Zhu X, Jacobsson G, Johansson BR, Geoghegan JA, Foster TJ, Josefsson E, Bylund J, Verhamme P, Jin T.** 2016. Staphylokinase Control of Staphylococcus aureus Biofilm Formation and Detachment Through Host Plasminogen Activation. J Infect Dis **213:**139-148.

91. **Cheng AG, Kim HK, Burts ML, Krausz T, Schneewind O, Missiakas DM.** 2009. Genetic requirements for Staphylococcus aureus abscess formation and persistence in host tissues. FASEB J **23:**3393-3404.

92. **Skaar EP, Humayun M, Bae T, DeBord KL, Schneewind O.** 2004. Iron-source preference of Staphylococcus aureus infections. Science **305:**1626-1628.

93. **Sebulsky MT, Hohnstein D, Hunter MD, Heinrichs DE.** 2000. Identification and characterization of a membrane permease involved in iron-hydroxamate transport in Staphylococcus aureus. J Bacteriol **182:**4394-4400.

94. **Nairz M, Haschka D, Demetz E, Weiss G.** 2014. Iron at the interface of immunity and infection. Front Pharmacol **5:**152.

95. **Nairz M, Dichtl S, Schroll A, Haschka D, Tymoszuk P, Theurl I, Weiss G.** 2018. Iron and innate antimicrobial immunity-Depriving the pathogen, defending the host. J Trace Elem Med Biol **48:**118-133.

96. **Szafranska AK, Oxley AP, Chaves-Moreno D, Horst SA, Rosslenbroich S, Peters G, Goldmann O, Rohde M, Sinha B, Pieper DH, Loffler B, Jauregui R, Wos-Oxley ML, Medina E.** 2014. High-resolution transcriptomic analysis of the adaptive response of Staphylococcus aureus during acute and chronic phases of osteomyelitis. MBio **5**.

97. **Date SV, Modrusan Z, Lawrence M, Morisaki JH, Toy K, Shah IM, Kim J, Park S, Xu M, Basuino L, Chan L, Zeitschel D, Chambers HF, Tan MW, Brown EJ, Diep BA, Hazenbos WL.** 2014. Global gene expression of methicillin-resistant Staphylococcus aureus USA300 during human and mouse infection. J Infect Dis **209:**1542-1550.

98. **Kothary V, Doster RS, Rogers LM, Kirk LA, Boyd KL, Romano-Keeler J, Haley KP, Manning SD, Aronoff DM, Gaddy JA.** 2017. Group B Streptococcus Induces Neutrophil
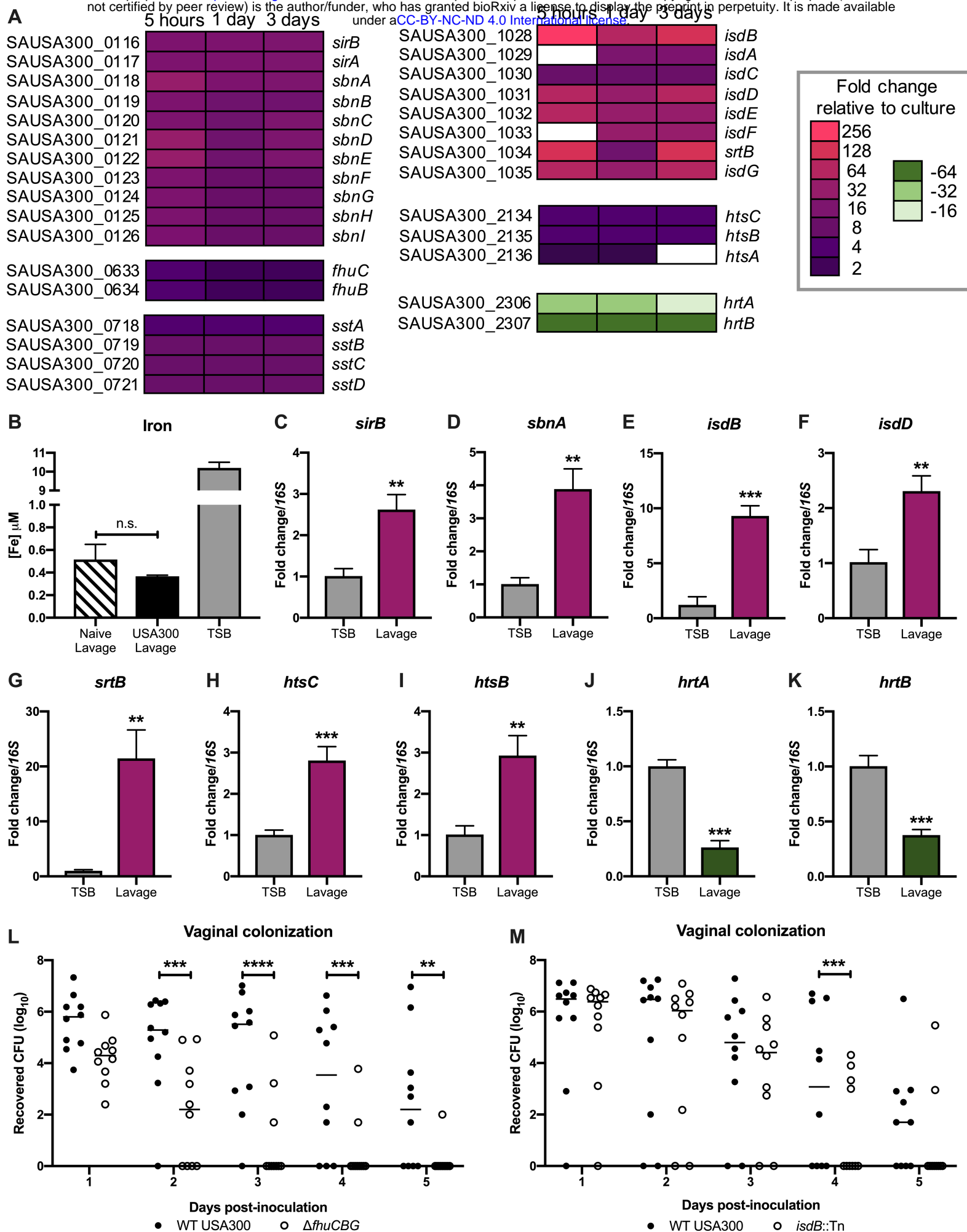
838   Recruitment to Gestational Tissues and Elaboration of Extracellular Traps and
839   Nutritional Immunity. Front Cell Infect Microbiol **7:**19.

840 99. **Zygiel EM, Nolan EM.** 2018. Transition Metal Sequestration by the Host-Defense Protein
841   Calprotectin. Annu Rev Biochem **87:**621-643.

842 100. **Jean S, Juneau RA, Criss AK, Cornelissen CN.** 2016. Neisseria gonorrhoeae Evades
843   Calprotectin-Mediated Nutritional Immunity and Survives Neutrophil Extracellular Traps
844   by Production of TdfH. Infect Immun **84:**2982-2994.

845 101. **Diaz-Ochoa VE, Jellbauer S, Klaus S, Raffatellu M.** 2014. Transition metal ions at the
846   crossroads of mucosal immunity and microbial pathogenesis. Front Cell Infect Microbiol
847   **4:**2.

848 102. **Novick RP.** 1991. Genetic systems in staphylococci. Methods Enzymol **204:**587-636.

849 103. **Wormann ME, Reichmann NT, Malone CL, Horswill AR, Grundling A.** 2011. Proteolytic
850   cleavage inactivates the Staphylococcus aureus lipoteichoic acid synthase. J Bacteriol
851   **193:**5279-5291.

852 104. **Nair D, Memmi G, Hernandez D, Bard J, Beaume M, Gill S, Francois P, Cheung AL.** 2011.
853   Whole-genome sequencing of Staphylococcus aureus strain RN4220, a key laboratory
854   strain used in virulence research, identifies mutations that affect not only virulence
855   factors but also the fitness of the strain. J Bacteriol **193:**2332-2335.

856 105. **Fey PD, Endres JL, Yajjala VK, Widhelm TJ, Boissy RJ, Bose JL, Bayles KW.** 2013. A
857   genetic resource for rapid and comprehensive phenotype screening of nonessential
858   Staphylococcus aureus genes. MBio **4:**e00537-00512.

859 106. **Olson ME.** 2016. Bacteriophage Transduction in Staphylococcus aureus. Methods Mol
860   Biol **1373:**69-74.

861 107. **Ibberson CB, Parlet CP, Kwiecinski J, Crosby HA, Meyerholz DK, Horswill AR.** 2016.
862   Hyaluronan Modulation Impacts Staphylococcus aureus Biofilm Infection. Infect Immun
863   **84:**1917-1929.

864 108. **Livak KJ, Schmittgen TD.** 2001. Analysis of relative gene expression data using real-time
865   quantitative PCR and the 2(-Delta Delta C(T)) Method. Methods **25:**402-408.

866

A USA300

B MRSA252

C USA300 day 1

D MRSA252 day 1

H&E   DAPI USA300

E Vagina

F

G Cervix

H

I Uterus

J

K Cervix

L Uterus

A Vaginal colonization

B Mean swab CFU
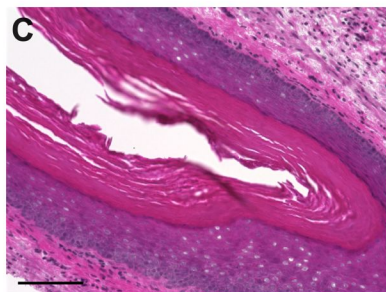
C — H&E (Naive)
D — Gr-1 (Naive)
E — H&E (Naive)
F — Gr-1 (Naive)
G — H&E (MRSA colonized)
H — Gr-1 (MRSA colonized)
I — H&E (MRSA colonized)
J — Gr-1 (MRSA colonized)
K — H&E (MRSA colonized)
L — Gr-1 (MRSA colonized)
M — H&E (MRSA colonized)
N — Gr-1 (MRSA colonized)
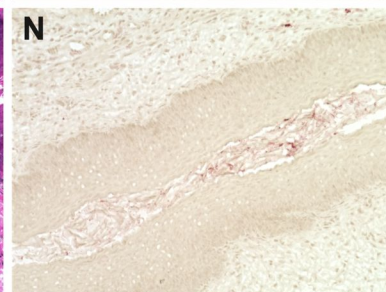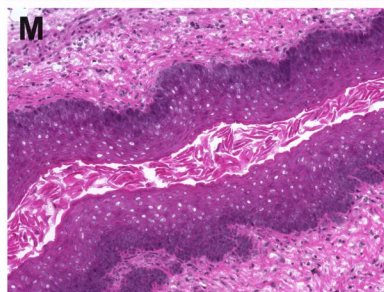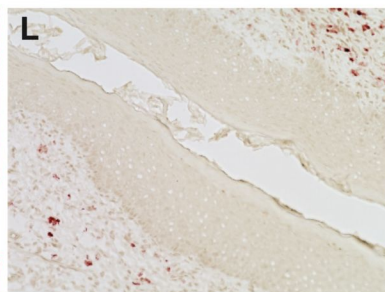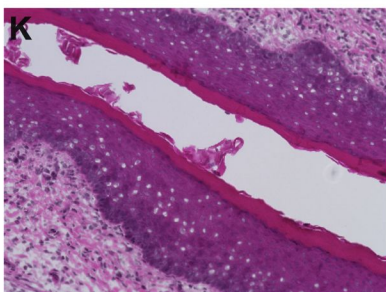
1-day post-inoculation

3-days post-inoculation

● USA300   ◉ MRSA252

A Fibrinogen

B VK2

C WT

D ΔclfA ΔfnbAB clfB::Tn ΔsdrCDE

E Ect1

F End1

G Vaginal colonization

Days post-inoculation

● WT USA300   ○ ΔclfA ΔfnbAB clfB::Tn ΔsdrCDE

Category	Locus_tag	Gene	Fold change		
			5 hours	1 day	3 days
transcriptional regulation	SAUSA300_0195	rpiRb	3	3	3
	SAUSA300_0218	hptS	3	3	4
	SAUSA300_0255	lytR	6	7	6
	SAUSA300_0878	LysR family transcriptional regulator	9	5	5
	SAUSA300_1220	LuxR family DNA-binding response regulator	2	2	2
	SAUSA300_1257	msrR	5	5	4
	SAUSA300_1514	fur	3	3	2
	SAUSA300_1717	arsR	7	4	5
	SAUSA300_1798	airR	4	4	4
	SAUSA300_1799	airS	3	4	4
	SAUSA300_2098	czrA	15	13	15
	SAUSA300_2300	TetR family transcriptional regulator	3	3	3
	SAUSA300_2322	TetR family transcriptional regulator	4	4	4
	SAUSA300_2336	MerR family transcriptional regulator	3	2	3
	SAUSA300_2347	nirR	12	8	7
	SAUSA300_2437	sarT	11	18	13
	SAUSA300_2566	arcR	4	4	6
	SAUSA300_2571	argR	3	4	6
	SAUSA300_2640	Xre family transcriptional regulator	5	9	11
toxins	SAUSA300_0800	sek	6	7	7
	SAUSA300_0801	seq	4	6	5
	SAUSA300_1058	hla	19	6	18
	SAUSA300_1918	truncated beta-hemolysin	14	2	9
extracellular enzymes	SAUSA300_0923	htrA	3	4	4
	SAUSA300_0951	sspA	2	12	13
	SAUSA300_1753	splF	12	3	24
	SAUSA300_1755	splD	13	5	28
	SAUSA300_1756	splC	11	3	22
	SAUSA300_1757	splB	12	4	21
	SAUSA300_2572	aur	4	15	12
ECM binding	SAUSA300_0546	sdrC	6	12	16
	SAUSA300_0547	sdrD	9	19	22
	SAUSA300_0774	empbp	35	4	8
immune modulation	SAUSA300_1059	superantigen-like protein	10	3	4
	SAUSA300_1060	superantigen-like protein	12	4	6
	SAUSA300_1061	superantigen-like protein	8	6	7
	SAUSA300_1920*	chs	29	3	8
	SAUSA300_0224*	coa			4
	SAUSA300_0836*	dltB			2
	SAUSA300_0837*	dltC			2
	SAUSA300_1053*	formyl peptide receptor-like 1 inhibitory protein			4
	SAUSA300_1055*	efb			2
	SAUSA300_2364*	sbi			2
type VII secretion system	SAUSA300_0279*	esaA			5
	SAUSA300_0280*	essA			2
	SAUSA300_0281*	esaB		4	4
	SAUSA300_0282	essB	2	6	6
	SAUSA300_0283*	essC		3	3
	SAUSA300_0284*	esxC		3	2
	SAUSA300_0286*	essE		3	3
	SAUSA300_0287*	esxD		3	3
	SAUSA300_0288*	essD		2	
	SAUSA300_0290	DUF5079 family protein	6	9	9
	SAUSA300_0291	DUF5080 family protein	5	7	6
	SAUSA300_0298	essI5	3	4	3
	SAUSA300_0299*	essI6		2	
	SAUSA300_0300*	essI7		2	2
	SAUSA300_0302	essI9	3	5	5
	SAUSA300_0303*	DUF4467 domain-containing protein		2	3